Chapter 3

Validation of forced convection heat transfer with variable density

1.1 Blasius Flow

Blasius type flows have been extensively studied in the past since it contains many of the main features found in turbulent boundary layers. It is often considered the cornerstone of viscous flows and is one type of canonical problem that has been useful over the years as a CFD benchmark since there exists an exact analytical solution.

The modeling of blasius type flows in LES3D-MP involves the development of inflow and outflow boundary conditions. An inflow boundary condition can be easily specified by providing stream-wise and vertical velocity profiles that are consistent with the blasius solution. On the other hand, outflow boundary conditions are challenging since we would like the code the compute the flow naturally. To do this, an Orlansky boundary condition [1] is utilized where a convective non-reflective boundary condition is applied. A transient hyperbolic wave equation is specified based on a convective velocity, Uc. The convective velocity can be specified as the mean or maximum velocity at the outflow boundary. For the simulations discussed in this chapter we have found very little differences using mean or maximum velocity so a conservative mean convective velocity is utilized.

$$\frac{\partial u_i}{\partial t_i} = -U_{conv} \frac{\partial u_i}{\partial x_i}$$

Mass conservation in LES3D-MP is enforced at all the interior nodes by the fractional step algorithm as was discussed in Chapter 2. Therefore, to prevent instabilities and unphysical wave propagations back into the domain a global mass conservation statement must be computed and also

enforced at the outflow. This is achieved by computing the mass flux across each boundary, flow dilatation and writing a conservation statement that will correct the scalars at the outflow. This is done by accounting for a conservation coefficient, alpha:

$$\alpha = \frac{\int \left(\rho u_{inflow}\right) dy - \int \left(\rho v_{top}\right) dx + \int \left(\rho v_{botom}\right) dx - \iiint \left(\frac{\partial \rho}{\partial t}\right) dxdydt}{\int \left(\rho u_{out}\right) dy}$$

The figure belows shows the spatial development of the skin friction coefficient compared to the blasius solution. The case corresponds to Reynolds number of 50 with a displacement thickness and velocity of unity chosen as the reference length and velocity scales. It is performed on a computational domain of X*=200, Y*=60, Z*=5.0 with a total of 50,000 grid cells that spatially resolve the boundary layer. Good agreement is found with blasius solution demonstrating the fidelity of the solver to capture boundary layer type problems.

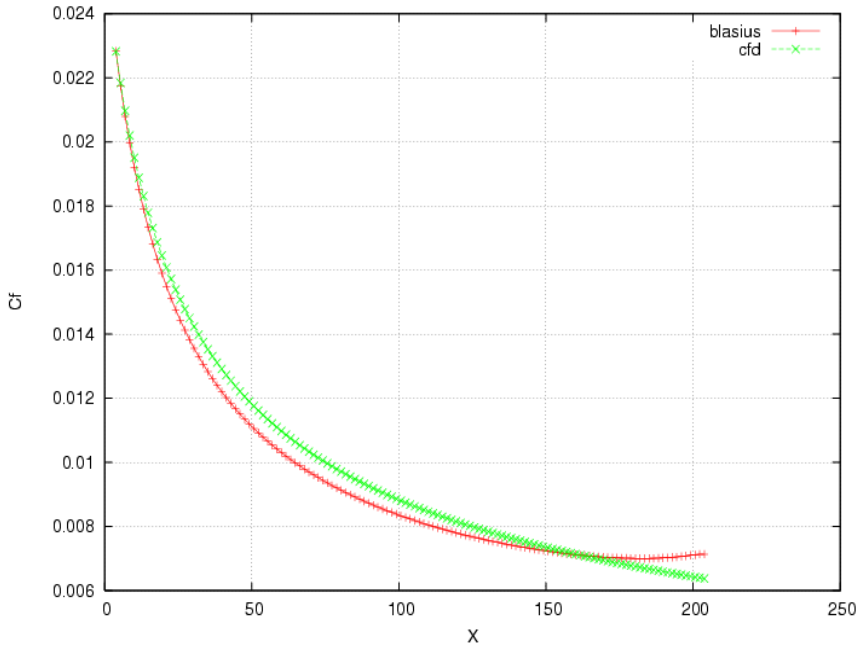

Illustration 1: Skin friction coefficient in Blasius flow (Re=50)

Variable density effects are considered by specifying an isothermal wall along the entire length of the plate. The flow properties in this case are Reynolds number of 50 and Prandlt number of 0.71 allowing the hydrodynamic and temperature boundary layers to have similar characteristics. The following figures show temperature contours of a successful simulation for cases where the normalized wall temperature are T* = 1.5 and T* = 2.0.

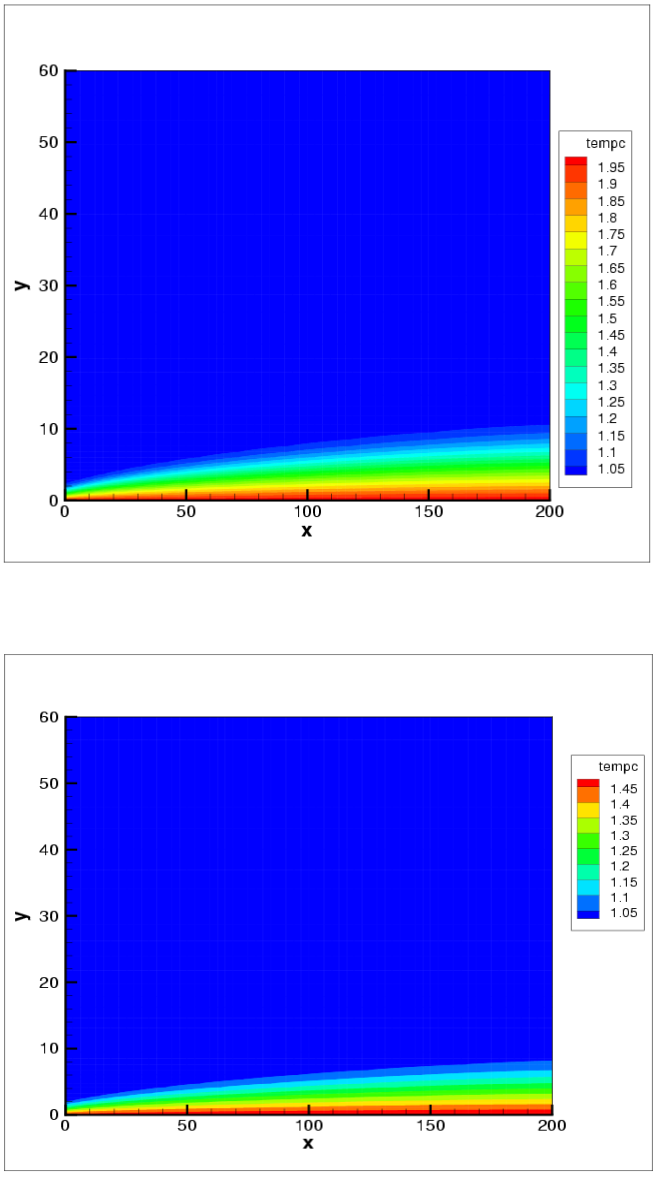

Illustration 2: Heat transfer with variable density in Blasius flow (Re=50, Pr= 0.71). (i) T= 1.5, (ii) T*=2.0.*

1.2 Poiseuille Flow

Another type of canonical flow extensively found in the literature is the classical Poiseuille flow. This class of problem deals with axial flows in channels or tubes where the fluid motion is driven by an axial pressure gradient. By assuming the channel is infinitely long the hydrodynamic and thermal entrance region can be neglected and thus an analytical solution of the governing equations may be easily obtained with simplifying assumptions.

When performing simulations, hydrodynamic entrance region effects can be computed or can be more conveniently bypassed by introducing the poiseuille solution at the inflow. In doing so we are implicitly specifying a dynamic viscosity and pressure gradient that can be serve for verification purposes. A similar Orlansky type outflow strategy is utilized for spatially developing conditions. The computational domain here is Lx= $2\pi\delta$, Ly= 2δ and Lz= $\pi\delta$ with a total number of 4100 grid cells for a Re =10. The following figures show a successful comparison with the theoretical velocity profile and pressure gradient.

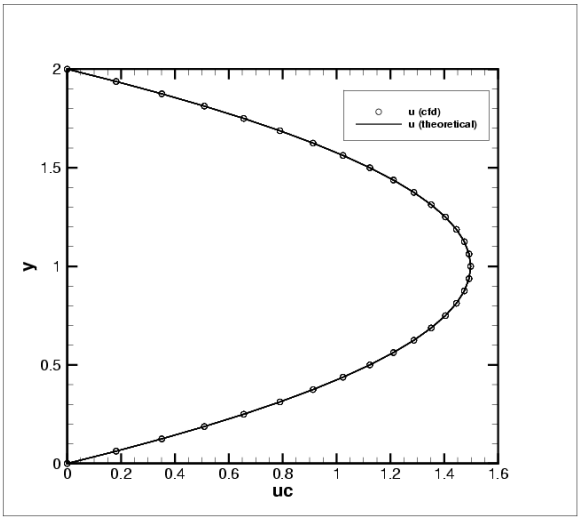

Illustration 3: Poiseuille Flow – velocity profile, Re = 10.

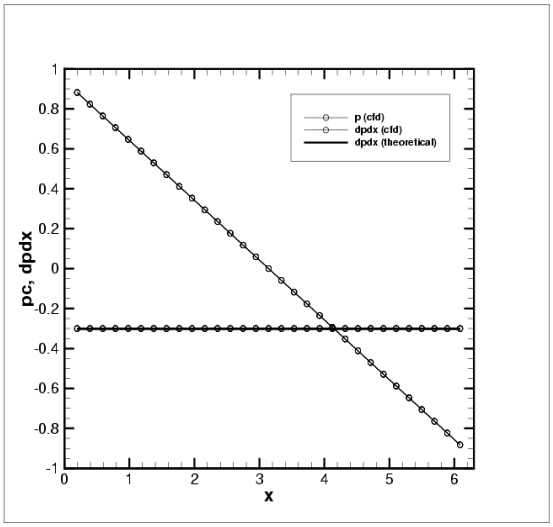

Illustration 4: Poiseuille Flow -- axial pressure profiles , Re = 10.

Heat transfer and variable density effects are considered by specifying isothermal boundary conditions in the wall-normal direction at y = 0 and y = 2 δ . A poiseuille profile and a uniform ambient temperature (T*=1) is specified at the inflow, x=0, to capture a thermal entrance region. The following scalar profiles show clean spatial development of the thermal boundary layers due to entrance region effects.

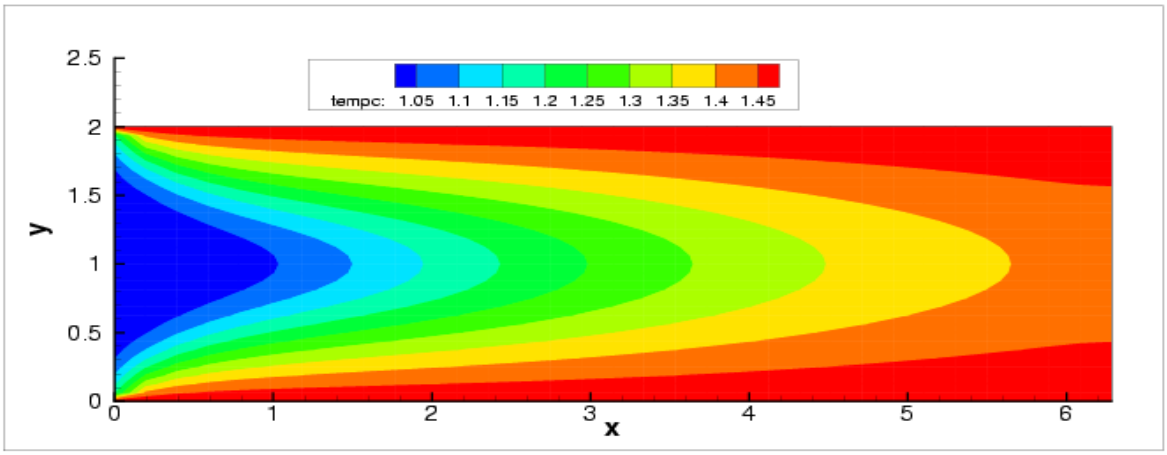

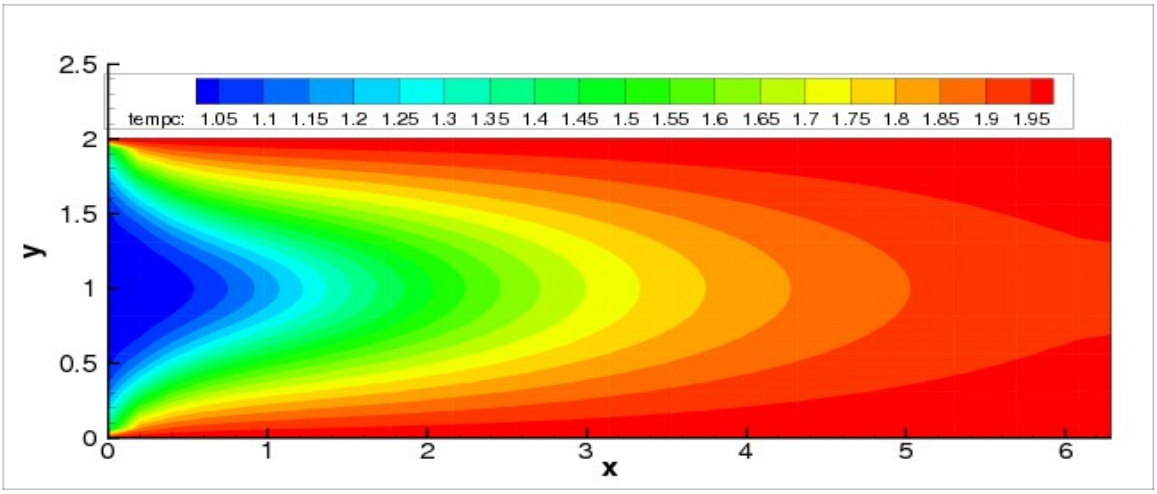

Illustration 5: Heat transfer with variable density in Poiseuille flow, Pr= 0.71. (i) T= 1.5, (ii) T*=2.0.*

1.3 Turbulent Channel Flow (Kim & Moser)

The classical work of Kim et al [2] is studied to show the advanced turbulence modeling capabilities of LES3D-MP. The current case corresponds to an incompressible turbulent channel with periodic boundary conditions in the stream-wise and span-wise directions and no-slip conditions on the wall normal direction. The Reynolds number used to characterize the flow is $Re = \delta \bar{U} / \nu$ where $\bar{U}$ is the bulk velocity and δ is the channel half height. As in the poiseuille case, the flow is driven by a pressure gradient which is modified at each time-step to keep the mass flux constant using the following equation:

$$\left(\frac{dp}{dx}\right)^{(n)} = \left(\frac{dp}{dx}\right)^{(n+1)} - 2\left(\frac{\dot{m}_{star}^{(n)} - \dot{m}}{dt}\right) - \left(\frac{\dot{m}_{star}^{(n-1)} - \dot{m}}{dt}\right)$$

where dp/dx is the mean pressure gradient imposed, $\dot{m}_{star}^{n}$ is the calculated mass flux at the current time level and $\dot{m}$ is the required mass flux. A successful simulation of this case requires an adequate grid to resolve the turbulent eddies generated in the near wall region. Quantities of interest are normalized by the friction velocity and the viscous length-scale defined by,

$$u_\tau = \sqrt{\frac{\tau_{wall}}{\rho}} = \sqrt{\nu \frac{\partial u}{\partial y}} \qquad \delta_\nu = \frac{\nu}{u_\tau}$$

where τ_{wall} is the wall shear stress and ρ is the density of the fluid. At the wall, the no-slip boundary condition dictates that all the Reynolds stresses are zero thus justifying that the wall shear stress is due entirely to the viscous contribution. The distance from the wall measured in viscous lengths (wall units) is defined by $y+ = y/\delta_\nu = u_\tau y/\nu$ where y+ plays a role similar to a local Reynolds number. In Large Eddy Simulations the standard resolution guideline to resolve the inner layer is to require the stream-wise and span-wise grid spacing to be dx+ ~ 100 and dz+ ~ 30 for spectral methods and half of that for low order finite difference solvers dx+ ~ 50 and dz ~ 15 (Piomelli et al). Additionally, the first grid point in the wall-normal direction must be able to resolve the sharp gradients in the viscous region,

thus y+ < 1 must be enforced.

When performing the simulation we allow the flow to reach a fully developed region in which velocity statistics no longer vary with increasing x. Hence the fully developed channel flow being considered is statistically stationary and statistically one dimensional, with velocity statistics depending only on *y.* A useful diagnostic to indicate a steady state regime is the total turbulent kinetic energy, which includes mean properties averaged in streamwise and spanwise directions,

$$tke = \frac{1}{2}\left(u_f^2 + v_f^2 + w_f^2\right)^{0.5}$$

A statistically stationary region is achieved once the turbulent kinetic energy has leveled off as is indicated in the figure below. Turbulent statistics can then be sampled by taking 10 data samples per large eddy turnover time (LETOT) defined by δ / u_τ where we perform a total sampling time of 10 LETOTS.

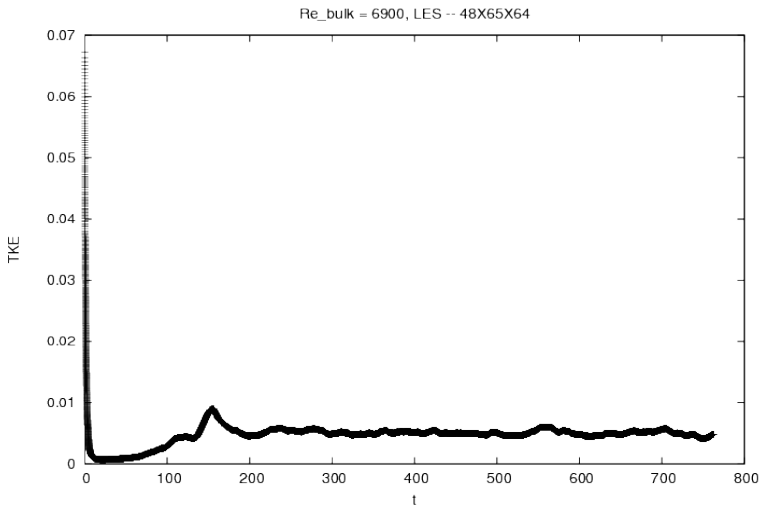

Illustration 6: Total turbulent kinetic energy, Re_tau = 395.

Results from a large-eddy simulation performed using the dynamic eddy viscosity model (DEV) are presented for a bulk Reynolds number of Re = 6900. The bottom and top walls are at y = 0 and y = 2 δ , respectively, with the mid-plane being at y= δ (channel half height). The stream-wise and span-wise computational domain lengths are 2π and π and the resolution is given by 48 x 65 x 64 in the x, y, and z directions. Mean velocity profiles in wall units show excellent agreement with the classical viscous and log law of the wall as well as DNS results (Figure 7). Typical LES modeling errors can be observed from Figure 8 where the Reynolds stress components are compared to DNS results.

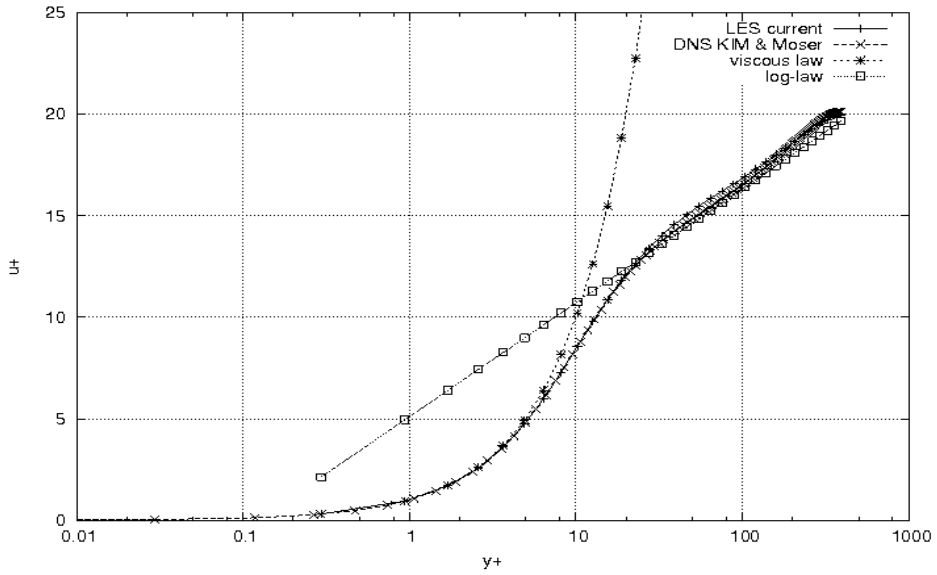

Illustration 7: Mean profiles normalized in viscous wall units for Re_tau =395. Viscous and log law of the wall are shown.

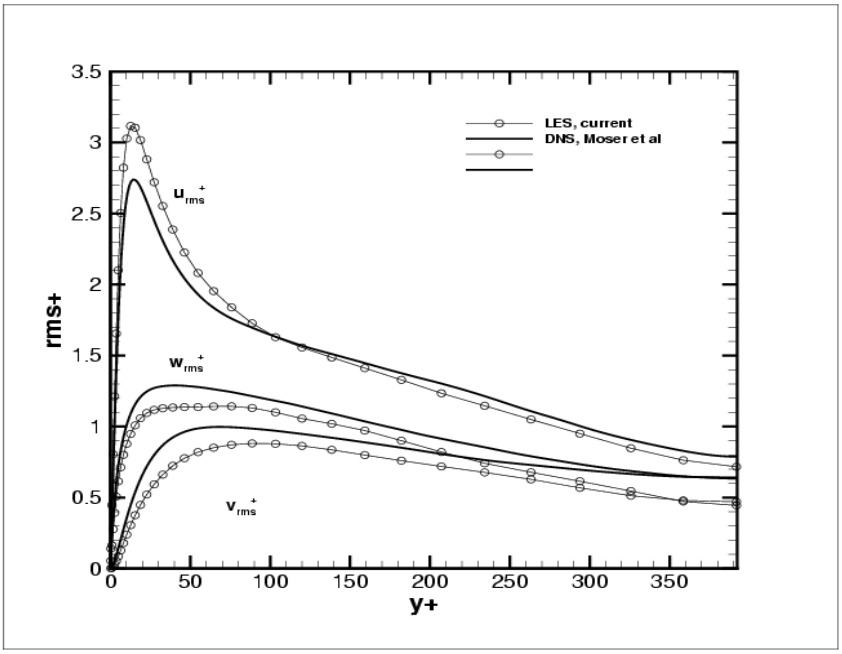

Illustration 8: Second order velocity rms profiles compared to DNS of Kim & Moser, Re_tau = 395.

1.5 Conclusions

Bibliography

[1] Orlansky, I; “A simple boundary condition for unbounded hyperbolic flows”, *Journal of Computational Physics*, ***21***, *1976*, *pg 251*.

[2] Pope, S; “Turbulent Flows”, *Cambridge University Pres*, *2001*.

[3] R. D. Moser, J. Kim, and N. N. Mansour, “Direct Numerical Simulation of Turbulent Channel Flow up to Re_tau = 590”, *Physics of Fuids*, Vol. 11, Nº 4, April 1994, pp. 943-945.

[4] Nicoud, F; “Conservative High Order Finite-Difference Schemes for Low Mach Number Flows” , *Journal of Computational Physics*, **158,** 2000 pg 71-97.